Factorisation issues in diffraction

A. Bunyatyan[a] *

[a]DESY, MPI für Kernphysik, Heidelberg and Yerevan Physics Institute

The high centre-of-mass energies of the HERA ep collider and of the Tevatron collider allow us to study the diffractive interactions in the presence of a hard scale and to describe them in terms of perturbative QCD. In QCD, the diffractive exchange is described in terms of partons, and the factorisation theorem states that the cross section for hard interactions can be expressed as convolution of universal diffractive parton distribution functions and process-dependent coefficients, perturbatively calculable. The recent experimental data from the H1 and ZEUS Collaborations at HERA are presented for diffractive dijet and D^* meson production, in both deep-inelastic scattering (DIS) and photoproduction regime and compared to next-to-leading order QCD predictions using diffractive parton distributions. While good agreement is found for dijets in DIS and for D^* production in both DIS and the photoproduction, the dijet photoproduction data are overestimated by NLO predictions at lower transverse momentum of the jets, indicating the breaking of QCD factorisation.

1. Introduction

A significant progress has been achieved over the last decade in understanding of diffractive phenomena at high energies in the light of measurements of hard diffractive processes at HERA. These processes, schematically represented in Figure 1, are identified experimentally by the presence of a final proton, tagged in the detectors at small angle, or by a large gap in rapidity between the system X of the outgoing hadrons and the proton remnant Y. In QCD, the probability to have no parton emission filling this rapidity gap is exponentially suppressed; the origin of these events is then due to a colourless exchange, referred to as Pomeron.

The variables used to describe the kinematics of inclusive diffractive events are the photon virtuality Q^2, the squared momentum transfer at the proton vertex $t = (p - p_Y)^2$, the fraction of longitudinal momentum transfer from the incoming proton to the system X, $x_{I\!P} = q(p - p_Y)/qp$ and the fraction of the exchanged momentum participating to the scattering with the photon, $\beta = x_{Bj}/x_{I\!P}$, where $x_{Bj} = Q^2/(2p \cdot q)$ is the Bjorken variable.

*Talk given at the Ringberg Workshop on New Trends in HERA Physics 2008

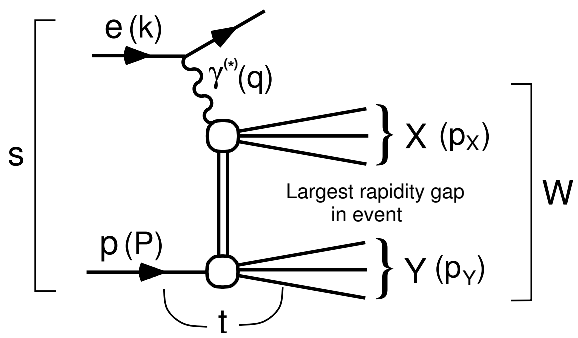

Figure 1. Illustration of the generic diffractive process $ep \to eXY$. The systems X and Y are separated by the largest gap in the rapidity distribution of the final state hadrons.

The central problem in hard diffraction is the question of the validity of *QCD factorisation.* In diffractive deep-inelastic scattering (DIS), the presence of a hard scale, as, for example, the photon virtuality Q^2, the large transverse jet momentum in the photon-proton centre-of-mass frame or the heavy-quark mass, ensures the validity of the QCD factorisation theorem. It allows the cross sections to be calculated as convolution of the

the partonic cross sections $\sigma^{\gamma^* i}$ and the universal diffractive parton densities functions (DPDFs) $f_i^D(x_{I\!P}, t, x, Q^2)$, that can be interpreted as the parton probability distribution in the proton conditional on the observation of a diffractive proton in the final state with a given t and $x_{I\!P}$:

$$\sigma^D(\gamma^* p \to Xp) \propto \sum_i f_i^D(x_{I\!P}, t, x, Q^2) \otimes \sigma^{\gamma^* i}(x, Q^2)$$

For diffractive DIS the QCD factorisation [1–4] has been proven by Collins [4], while it is expected to break down for hard processes in diffractive hadron-hadron scattering, due to rescattering of hadronic remnants (see e.g. [1]). These interactions occur in both the initial and final state and destroy the rapidity gap. A 'gap survival probability' factor must therefore be included in diffractive hadron-hadron scattering cross section calculations based on DPDFs. Factorisation breaking has been observed in $p\bar{p}$ collisions at the Tevatron: predictions using the DPDFs determined at HERA (as described in Section 3) overestimate the diffractive dijet cross sections measured by CDF by up to an order of magnitude [5]. All diffractive processes at the LHC are affected by rescatetring of hadronic remnants, with survival probabilities estimated to be no more than a few percent [6]. Understanding of the detailed physics of gap destruction is thus vital to the preparations for diffractive studies at the LHC.

QCD factorisation can be further tested at HERA in diffractive photoproduction ($Q^2 \sim 0$) of dijets or D^*. In these processes the validity of pQCD is ensured by the hard scale provided by the jet transverse energy or by the mass of c-quark. Processes in which the photon participates directly in hard scattering are expected to be similar to the deep-inelastic scattering of highly virtual photons ('point-like' or 'direct' photon, see Figure 2a). In contrast, processes in which the photon is resolved into partons which participate in hard scattering ('resolved' photon, see Figure 2b) resemble hadron-hadron scattering. In resolved photoproduction rescattering of the photon remnant may lead to breaking of QCD factorisation. A suppression by about a factor of three for resolved photoproduction at HERA is predicted [7]. In QCD, the direct and the resolved processes is unambiguously distinguished only in leading order (LO). In next-to-leading order (NLO) these two processes are related and the separation depends on the factorisation scheme and scale. Experimentally, a rough separation of the direct and the resolved processes can be made via the x_γ variable, an estimator of the fraction of the photon energy participating in the hard scattering.

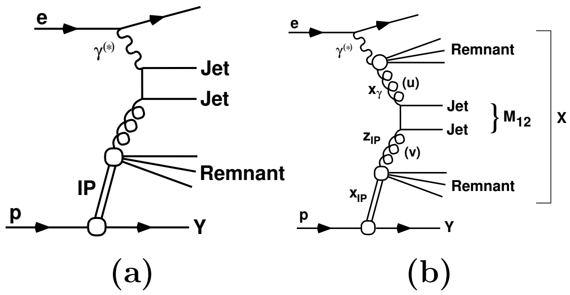

Figure 2. Leading order diagrams for diffractive dijet production at HERA. (a) direct (pointlike) processes, (b) resolved (hadron-like) photon process.

In addition, it is important to test a conjecture of *Regge (proton vertex) factorisation*, which assumes that the diffractive cross section can be expressed as a product of Pomeron flux and its structure function [8]:

$$f_i^D(x_{I\!P}, t, x, Q^2) = f_{I\!P/p}(x_{I\!P}, t) \times f_i^{I\!P}(\beta = x/x_{I\!P}, Q^2)$$

In this report both the hard QCD and the Regge factorisation hypothesis are confronted with the recent HERA data.

2. Test of Regge factorisation in inclusive diffraction

One of the basic predictions in Regge model is a specific asymptotic behavior of the total, elastic and diffractive cross sections with energy, which is controlled by the value of intercept of the universal Pomeron trajectory, $\alpha_{I\!P}(t)$ at $t = 0$. If Regge factorisation holds, the Pomeron flux, parameterised as $f_{I\!P/p}(x_{I\!P}, t) \propto x_{I\!P}^{1-2\alpha_{I\!P}(t)} e^{bt}$, should not depend on β and Q^2.

Figure 3 shows the Q^2 dependence of the diffractive structure function $x_{I\!P} F_2^{D(3)}$ (defined in section 3) for fixed β and $x_{I\!P}$, measured by ZEUS [9]. It can be seen, that for a fixed bin of β the shape of Q^2 distribution shows dependence on the value of $x_{I\!P}$. This observation contradicts the assumption of Regge factorisation.

On the other hand, no indication of Regge factorisation breaking is observed in H1 data [10].

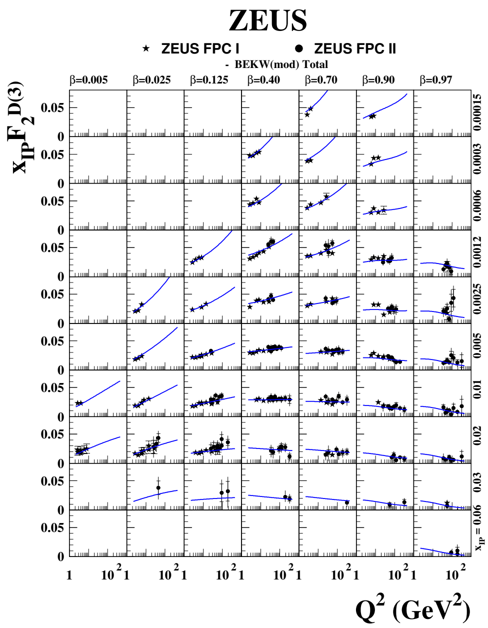

Figure 3. The diffractive structure function of the proton, $x_{I\!P} F_2^{D(3)}$, as a function of Q^2 for different regions of β and $x_{I\!P}$ from the ZEUS data [9].

3. Partonic structure of the diffractive exchange

Diffractive PDFs have been determined at HERA from high-precision measurements of the inclusive diffractive DIS processes [5,9,11–14]. In analogy with non-diffractive DIS scattering, the cross section for neutral current events is proportional to the diffractive structure function $F_2^{D(4)}(Q^2, x_{I\!P}, \beta, t)$, neglecting the longitudinal contribution:

$$\frac{d^4\sigma(ep \to eXp)}{dQ^2 dx_{I\!P} d\beta dt} = \frac{4\pi\alpha^2}{\beta Q^4}(1-y+\frac{y^2}{2}) F_2^{D(4)}(Q^2, x_{I\!P}, \beta, t)$$

where $y = Q^2/(s \cdot x_{Bj})$ is the inelasticity variable. Assuming factorisation of the proton vertex, diffractive structure function is written as the product of the Pomeron flux factor $f_{I\!P/p}(x_{I\!P}, t)$ and the Pomeron structure function $F_2^{I\!P}(\beta, Q^2)$

$$F_2^{D(4)}(Q^2, x_{I\!P}, \beta, t) = f_{I\!P/p}(x_{I\!P}, t) \times F_2^{I\!P}(\beta, Q^2)$$

This assumption is a useful approximation. As discussed in section 2, a certain violation of Regge factorisation is observed in ZEUS data [9]. The fits to inclusive diffractive cross sections, described below, are however insensitive to this mild breaking.

When the scattered proton is not detected, the t-integrated diffractive structure function $F_2^{D(3)}$ is obtained via:

$$\frac{d^3\sigma(ep \to eXp)}{dQ^2 dx_{I\!P} d\beta} = \frac{4\pi\alpha^2}{\beta Q^4}(1-y+\frac{y^2}{2}) F_2^{D(3)}(Q^2, x_{I\!P}, \beta)$$

By analogy to the proton structure function F_2, the partonic distributions of the diffractive exchange are extracted from the Q^2 evolution of F_2^D. The gluon and singlet quark density are parameterised as a function of z, the Pomeron momentum fraction carried by the parton entering the hard interaction, at starting scale of $Q_0^2 = 2$ GeV^2 evolved in Q^2 using the DGLAP equations and fitted to the data [5].

The diffractive quark density and the gluon density at low to moderate z are well constrained from the inclusive cross sections alone. However, the sensitivity to the gluon density from the inclusive process is lost at large z, which is among the most important regions for LHC studies. The lack of a constraint on the high z gluon density is reflected e.g. in two different solutions of the DGLAP QCD fit to H1 data, 'H1 2006 fit A' and 'H1 2006 fit B', which differ only in the parameterisations of the gluon density at the starting

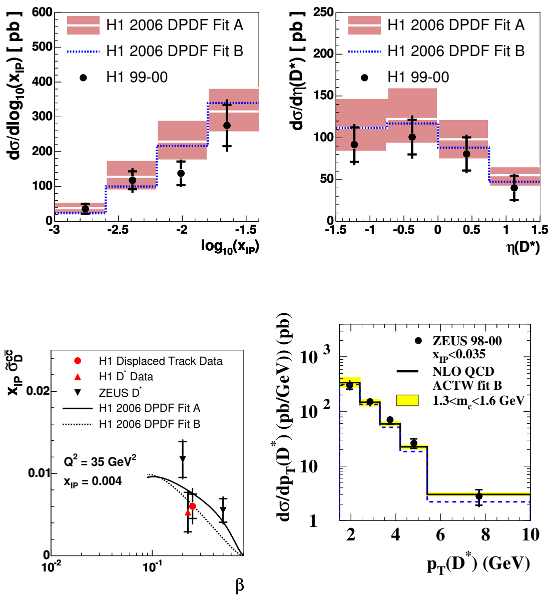

Figure 4. Differential cross sections for diffractive D^* meson production in DIS [16,17].

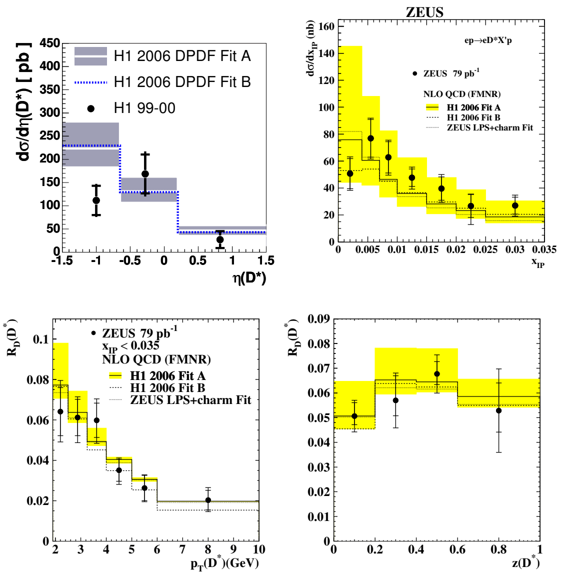

Figure 5. Differential cross sections for diffractive D^* meson photoproduction (upper plots) as well as the ratios of diffractive to inclusive D^* production (lower plots) [16,18].

scale (see Fig.10). Other available sets of parameterisations of DPDFs, which are also used in the comparisons in this report, are 'MRW' [15], obtained from the fit to H1 data from [5], and 'ZEUS LPS+charm fit' from the combined fit to ZEUS leading proton spectrometer and $F_2^{D,charm}$ data [11].

Production of hadronic final states in diffractive interactions, e.g. the open charm and dijet production, are directly sensitive to the diffractive gluon density via the boson-gluon fusion process $\gamma^* g \to q\bar{q}$. These measurements not only help to test the existing parameterisations, but also provide additional constraint of gluon density, in particular, at large z.

4. Diffractive D^* production in DIS and Photoproduction

The diffractive production of open charm has been studied by the H1 and ZEUS Collaborations [16–18]. The charm quark was tagged by the reconstruction of $D^*(2010)$ meson in DIS and photoproduction regimes. The H1 Collaboration used also the method based on the measurement of the displacement of tracks from primary vertex.

The measurements are compared with the NLO QCD predictions using the DPDFs extracted from the fits to the diffractive DIS cross sections from H1 and ZEUS. The calculations are performed using HVQDIS [19] for DIS and FMNR [20] for photoproduction. If QCD factorisation is valid, these calculations should be able to predict the production rates of open charm production in shape and normalisation.

In Figure 4 the cross sections are shown as function of $x_{I\!P}$, β and $p_T(D^*)$ in DIS. As seen from the figure, the NLO QCD calculations provide a good description of the measurements within the experimental and theoretical uncertainties.

In Figure 5 results of the measurements of diffractive D^* production in photoproduction regime are shown. As in DIS case, there is a fair agreement between the measurements and the calculations. The two lower plots of Figure 5 show the ratio of diffractive to inclusive D^* production cross sections. The average value of this ratio is $R_D = 5.7 \pm 0.5\%$. This number is good agreement with the values obtained from the NLO QCD calculations using the H1 2006 fit B (5.7%) and using the ZEUS LPS+charm fit (5.8%).

Thus, the NLO calculations provide satisfactory description of diffractive D^* data, both in DIS and photoproduction, supporting the validity if QCD factorisation.

5. Diffractive jet production in DIS

Diffractive jet production in DIS has been studied by both the H1 and ZEUS Collaborations [21–23]. The kinematic range of the photon virtuality is $4 < Q^2 < 80$ GeV^2 for H1 and $5 < Q^2 < 100$ GeV^2 for ZEUS analyses. Diffractive events are selected by requiring a large rapidity gap and the jets are identified using the longitudinally invariant inclusive k_T clustering algorithm in the photon-proton rest frame. The transverse energies for the two must energetic jets are required to be $E_{T,1}^{jet} > 5$ GeV and $E_{T,2}^{jet} > 4$ GeV, respectively.

The experimental results are compared to the NLO predictions obtained with the DISENT [24] and NLOJET++ [25] codes using different sets of DPDFs described in section 3.

The cross sections measured by H1 and ZEUS are shown in Figures 6 and 7, respectively. In general, the shapes of the measured cross sections are described by NLO calculations within the theoretical uncertainties, except at high value of $z_{I\!P}^{jets}$, an estimator of the fraction of the momentum of the diffractive exchange carried by the parton participating in the hard scattering. These results support the validity of QCD factorisation for diffractive dijet production within uncertainties.

The diffractive dijet data are sensitive to the choice of diffractive PDFs used in NLO QCD calculations. The best agreement is obtained by the predictions using DPDFs from H1 2006 fit B and MRW 2006– the DPDFs which have somewhat lower gluon component. This is also demonstrated in Figure 8 where the cross section is

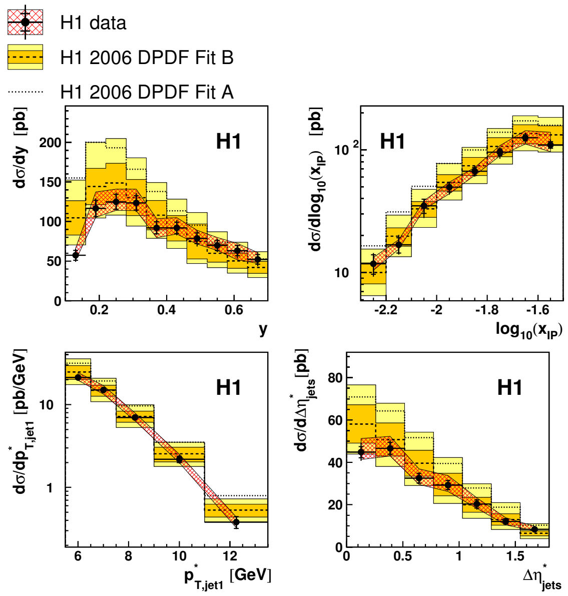

Figure 6. Differential cross sections of diffractive dijet production in DIS measured by H1 [21]. NLO predictions for several DPDFs parameterisations are compared to the measurements. The shaded bands show the uncertainty resulting from the variation of renormalisation scale.

shown a function of $z_{I\!P}^{jet}$ and is compared separately with the calculations using the fits from H1 2006 fit A and H1 2006 fit B. In [22] the diffractive dijet cross sections have been used together with the inclusive diffractive cross sections [5] in a combined NLO QCD fit. The result of combined fit, defined as 'H1 2007 Jets DPDF', is compared to the diffractive dijet data in Figure 9. This DPDF is able to describe well both the dijet and inclusive diffractive DIS data. The diffractive gluon and singlet quark distributions resulting from the fit are shown in Figure 10 together with the results of the fits H1 2006 fit A and H1 2006 fit B [5]. The gluon and quark components are determined with a good accuracy over the whole phase space, in particular in the range $0.05 < z_{I\!P} < 0.9$.

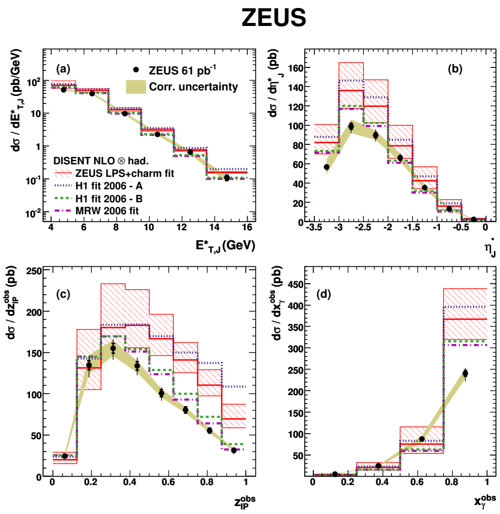

Figure 7. Differential cross sections of diffractive dijet production in DIS measured by ZEUS [23]. NLO predictions for several DPDFs parameterisations are compared to the measurements. The shaded bands show the uncertainty resulting from the variation of renormalisation scale.

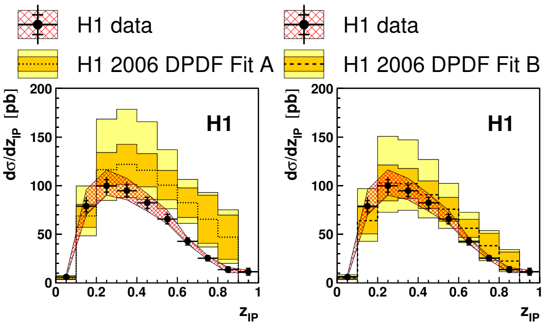

Figure 8. Differential cross sections of diffractive production of dijets in DIS as measured by H1 as function of $z_{I\!P}$ [21]. NLO predictions using H1 2006 fit A and H1 2006 fit B DPDFs parameterisations are compared to the measurements. The shaded bands show the uncertainty resulting from the variation of renormalisation scale.

6. Diffractive jet photoproduction

The diffractive photoproduction of dijets was analysed by both the H1 and ZEUS Collaborations [21,26,27]. The kinematic range of the H1 measurements is similar to the DIS measurements, i.e. $E_{T,1}^{jet} > 5$ GeV and $E_{T,2}^{jet} > 4$ GeV, while the ZEUS analysis required higher jet energies: $E_{T,1}^{jet} > 7.5$ GeV and $E_{T,2}^{jet} > 6.5$ GeV. Jets are identified using the inclusive k_T clustering algorithm in the laboratory frame.

The cross sections as function of $z_{I\!P}$ and x_γ measured by H1 are shown in Figure 11. The cross section measured as function of x_γ by ZEUS is shown in Figure 12. The measurements are compared with the NLO QCD predictions which are obtained using several DPDFs and photon PDFs parameterisations with two different programs, by Frixione and Ridolfi [28] and by Klasen and Kramer [29]. The both calculations lead to identical results. The NLO predictions have large uncertainties due to different DPDFs and due to the uncertainty in the renormalisation and factorisation scales. They are generally able to describe the shape of the distributions. The NLO calculations are $\sim$ 10–20% higher but compatible with ZEUS data (Figure 12). However, in order to describe the H1 measurements, the NLO QCD predictions need to be downscaled by a global-factor 0.5, as seen from Figure 11. Both experiments observe that the approach when only resolved photon part of the cross section is suppressed ($x_\gamma \lesssim 0.8$) is clearly disfavored by data in contradiction with theoretical expectation of [7]. This can be seen from the lower plot of Figure 12, where the NLO expectations are shown with the predicted resolved photon component scaled down by a factor of 0.34, according to [7].

The different conclusions of the both experiments on the size of suppression factor initiated detailed investigations. As a possible reason for this contradiction the difference in the kinematic region (E_T^{jet} range) of both measurements was suggested. In this case the suppression may depend on the E_T^{jet}. Indeed, double ratio of data cross section and NLO prediction for diffractive photoproduction and DIS as a function of transverse momentum E_T of the leading jet measured by H1 (upper plot of Figure 13) and the ratio of

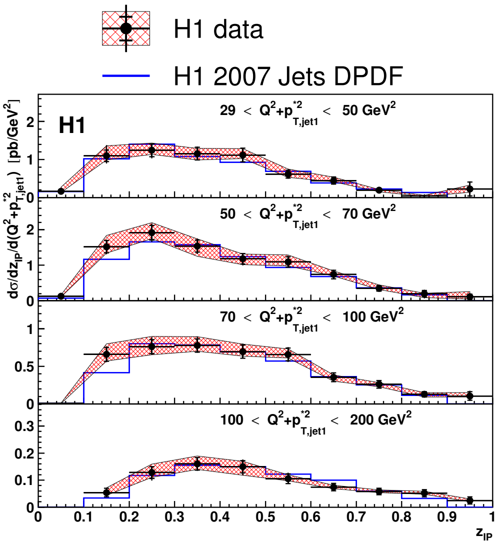

Figure 9. Cross section for diffractive dijet production doubly differential in $z_{I\!P}$. The solid line shows the NLO QCD prediction based on the H1 2007 Jets DPDF [21].

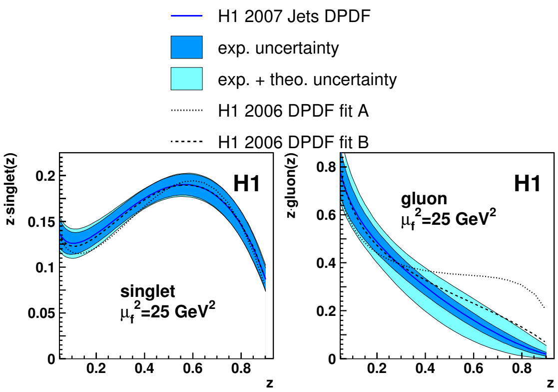

Figure 10. The diffractive quark and gluon densities for the squared factorisation scale $\mu_f^2 = 25$ GeV^2 [21]. The solid line indicates the H1 2007 Jets DPDF, surrounded by the experimental and theoretical uncertainties added in quadrature. The dotted and dashed lines show the parton densities corresponding to the H1 2006 fit A and B, respectively.

the ZEUS data cross section over the NLO predictions (lower plot of Figure 13), indicate the rise with increasing of E_T^{jet}.

A detailed study of this issue was performed in the new H1 analysis of dijets in photoproduction [27], in which two E_T^{jet} cut schemes were applied. The first scheme is identical to [21] with $E_{T,1} > 5$ GeV, to crosscheck results of previous analysis. The second scheme applies the cuts similar to ones used by ZEUS [26], in particular $E_{T,1}^{jet} > 7.5$ GeV, to check for a possible dependence of cross section suppression from E_T of the jets. In Figure 14 the results are compared to NLO calculations using three H1 DPDF fits: H1 2006 fit A, H1 2006 fit B and H1 2007 Jets. The best agreement of the shapes of measured cross sections was obtained with NLO predictions using H1 2006 fit B scaled by factor $0.54 \pm 0.01(\text{stat.}) \pm 0.10(\text{syst.}) \pm 0.14(\text{scale unc.})$ for low E_T cut scenario, and by factor $0.61 \pm 0.03(\text{stat.}) \pm 0.13(\text{syst.}) \pm 0.16(\text{scale unc.})$ for high E_T cut scenario. With higher E_T^{jet} cut the H1 data requires lower suppression, i.e. is closer to ZEUS result, obtained in this E_T range (with suppression factor of ~ 0.8).

The data show no evidence for a suppression as a function of x_γ. In the H1 analysis the comparison is made with NLO predictions for which only resolved part was suppressed by a factor 0.3 [7]. Also with this suppression scheme the several data distributions can be reasonably well described, both for lower E_T cut and higher E_T cut scenario. However, this leads to much worse description of x_γ distribution, in particular the NLO prediction clearly underestimates the data at lower x_γ and overestimates at $x_\gamma > 0.8$. This result is in qualitative agreement with the theoretical analysis of [29]. Thus, the suppression of the resolved component only is not favoured by data.

7. Dijet production with leading neutrons

Factorisation breaking is expected not only in the diffractive region, where the momentum fraction transferred to the exchanged particle in the t channel $x_{I\!P} \ll 1$, but also for events with larger

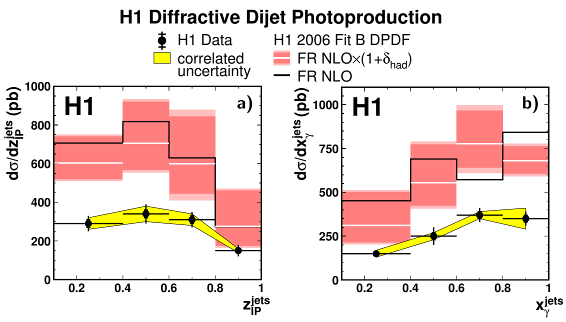

Figure 11. Differential cross section for the diffractive photoproduction of dijets as function of $z_{I\!P}$ and x_γ measured by H1 [22]. The NLO predictions of the Frixione et al. program interfaced to the H1 2006 Fit B DPDFs are also shown. The shaded bands show the uncertainty resulting from the variation of renormalisation scale.

values of $x_{I\!P}$ where Regge exchanges other than the Pomeron occur at the proton vertex. It is expected also for events with transition $p \to n$, dominated by the pion exchange (see diagram in Figure 15). Dijet photoproduction with a leading neutron $\gamma p \to jet + jet + n + X$ has been investigated to test factorisation breaking [31]. In these events soft rescattering is expected between the photon remnant and the neutron reducing the normalisation of the cross section.

The NLO QCD calculations [31] for dijet production with final state forward neutron are compared with the measured cross section in both the DIS and photoproduction regimes [32]. In this analysis jets are identified using the cone algorithm and selected by requiring $E^{jets}_{T,1(2)} > 7\ (6)$ GeV. In the pion exchange model, the cross section for leading neutron production is the product of the non-perturbative pion flux factor, describing the splitting function of a proton into a pion and a neutron, and the parton distribution function of the pion. In [31] the pion flux normalisation factor for the dijet photoproduction cross section was determined from the measurement of the DIS dijet cross section, where no absorptive interactions is expected. Figure 16 shows the cross sections for neutron-tagged dijet

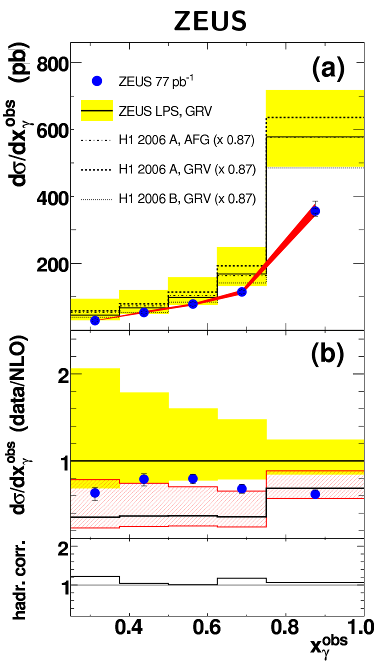

Figure 12. Differential cross section as a function of x_γ compared with NLO QCD predictions using the DPDFs from the ZEUS LPS+charm fit, the H1 2006 fit A and the H1 2006 fit B [26]. The lower plot shows the ratio of data and NLO predictions using the ZEUS LPS+charm fit. The histogram indicates the theory expectation with the resolved photon component scaled down by a factor of 0.34. The shaded and hatched bands show the theoretical uncertainty.

production in DIS and in photoproduction as a function of jet pseudorapidity. There is a good agreement between the NLO calculation and the measured cross sections in DIS regime. On the other hand, the NLO can describe the photoproduction measurement only after suppressing the resolved photon process by a factor of 0.48, or suppressing both the direct and resolved components by 0.64.

8. Conclusions

Diffractive processes have been extensively studied in ep interactions at HERA and the valid-

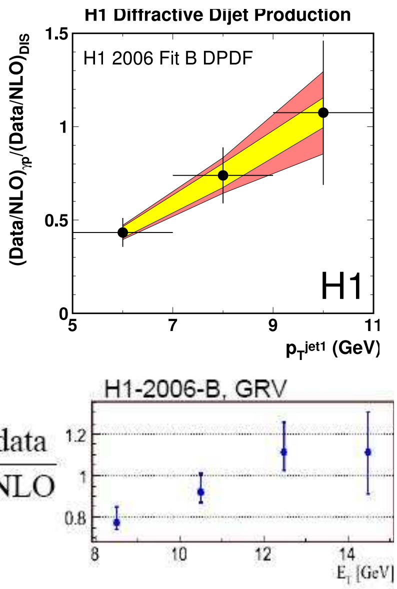

Figure 13. (Upper plot) Double ratio of cross section for the data and to NLO prediction for photoproduction and DIS as a function of transverse momentum of the leading jet measured by H1 (plot derived from [22]); (lower plot) ratio of cross sections of data and NLO for the diffractive photoproduction of dijets vs E_T of the leading jet as measured by ZEUS [30].

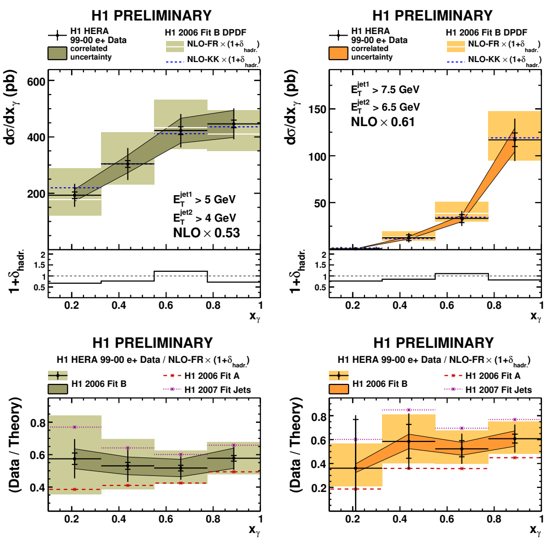

Figure 14. Differential cross sections for the diffractive photoproduction of dijets as a function of x_γ for the lower E_T cut scenario (left side plot) and higher E_T cut scenario (right side plot), as measured by H1 [27], compared with NLO calculation.

ity of the QCD factorisation theorem has been investigated. NLO predictions using the diffractive PDFs measured in inclusive diffraction successfully describe diffractive dijet and charm production in DIS, as well as charm photoproduction. In diffractive dijet photoproduction the situation is much less clear. The dijet photoproduction data are overestimated by NLO predictions at lower transverse momentum of the jets, indicating the breaking of QCD factorisation. Contrary to the theoretical expectations, no suppression is observed for the resolved component of the photon with respect to the direct component, while there is an indication of the dependence of the suppression factor on the transverse momenta of the jets. Similar suppression is also observed for dijet photoproduction with leading neutrons.

Acknowledgments

I would like to thank organizers for this interesting, stimulating and enjoyable workshop.

REFERENCES

1. A. Berera and D.E. Soper, *Phys. Rev.* **D 50** (1994) 4328.
2. L. Trentadue and G. Veneziano, *Phys. Lett.* **B 323** (1994) 201.
3. Z. Kunszt and W.J. Stirling, *"Hard diffractive scattering: Partons and QCD"*, ETH-TH-96-27, [hep-ph/9609245].
4. J.C. Collins, *Phys. Rev.* **D 57** (1998) 3951, [Erratum-ibid. D61, 019902 (2000).]
5. H1 Collaboration, A.Aktas *et al.*, *Eur. Phys. J.* **C 48** (2006) 715.
6. V.A. Khoze, A.D. Martin and M.G. Ryskin, *Eur. Phys. J.* **C 23** (2002) 311.
7. A.B. Kaidalov, V.A. Khoze, A.D. Martin and M.G. Ryskin, *Phys. Lett.* **B 567** (2003) 61.

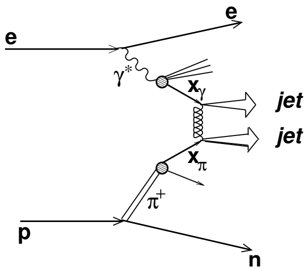

Figure 15. Generic Feynman diagram for the production of two jets in the one-pion exchange model.

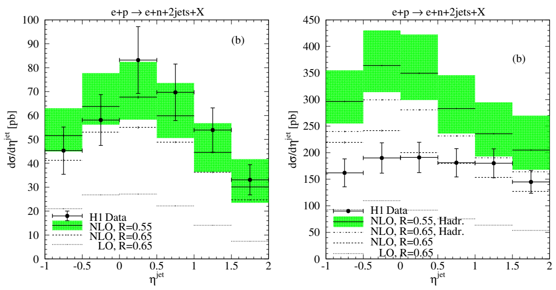

Figure 16. Differential cross sections for dijet production with a leading neutron in DIS (left) and photoproduction (right). The H1 measurement [32] is compared to perturbative QCD predictions in LO and NLO [31].

8. G. Ingelman and P. Schlein, *Phys. Lett.* **B 152** (1985) 256.
9. ZEUS Collaboration, S.Chekanov it et al., *Nucl. Phys.* **B 800** (2008) 1.
10. H1 Collaboration, A.Aktas *et al.*, *Eur. Phys. J.* **C 48** (2006) 749.
11. ZEUS Collaboration, S.Chekanov *et al.*, *Eur. Phys. J.* **C 38** (2004) 43.
12. H1 Collaboration, A.Aktas *et al.*, *Eur. Phys. J.* **C 48** (2006) 749.
13. ZEUS Collaboration, S.Chekanov *et al.*, *Nucl. Phys.* **B 713** (2005) 3.
14. ZEUS Collaboration, *"A study of inclusive diffraction in events with a large rapidity gap and with a leading protons"*, ZEUS-prel-06-024.
15. A.D. Martin, M.G. Ryskin and G. Watt, *Phys. Lett.* **B 644** (2006) 131.
16. H1 Collaboration, A.Aktas *et al.*, *Eur. Phys. J.* **C 50** (2007) 1.
17. ZEUS Collaboration, S.Chekanov *et al.*, *Nucl. Phys.* **B 672** (2003) 3.
18. ZEUS Collaboration, S.Chekanov *et al.*, *Eur. Phys. J.* **C 51** (2007) 301.
19. B.W. Harris and J. Smith, *Nucl. Phys.* **B 452** (1995) 109.
20. S. Frixione, M. Mangano, P. Nason and G. Ridolfi, *Phys. Lett.* **B 348** (1995) 633,
S. Frixione, P. Nason and G. Ridolfi, *Nucl. Phys.* **B 454** (1995) 3.
21. H1 Collaboration, A.Aktas *et al.*, JHEP **10**,042 (2007).
22. H1 Collaboration, A.Aktas *et al.*, *Eur. Phys. J.* **C 51** (2007) 249.
23. ZEUS Collaboration, S.Chekanov *et al.*, *Eur. Phys. J.* **C 52** (2007) 813.
24. S. Catani and M.J. Seymour, *Nucl. Phys.* **B 485** (1997) 291, Erratum:*ibid.* **B510**, 503 (1998).
25. Z. Nagy and Z. Trocsnyi, *Phys. Rev. Lett.* **87** (2001) 082001.
26. ZEUS Collaboration, S.Chekanov *et al.*, *Eur. Phys. J.* **C 55** (2008) 177.
27. H1 Collaboration, *"Diffractive photoproduction of jets with the H1 detector"*, H1prelim-08-012.
28. S. Frixione, Z. Kunszt and A. Signer, *Nucl. Phys.* **B 467** (1996) 399; S. Frixione and G. Ridolfi, *Nucl. Phys.* **B 507** (1997) 315.
29. M. Klasen and G. Kramer, *Eur. Phys. J.* **C 38** (2004) 93; *Mod. Phys. Lett.* **A23** (2008) 1885; *"Survival probability in diffractive dijet photoproduction"*, LPSC-08-115, arXiv:0808.3700 [hep-ph].
30. W. Slominski, *"Dijets in diffractive DIS and photoproduction"*, in XVI International Workshop DIS-2008, Apri 2008, London.
31. M. Klasen and G. Kramer, *Eur. Phys. J.* **C 49** (2007) 957.
32. H1 Collaboration, A.Aktas *et al.*, *Eur. Phys. J.* **C 41** (2005) 273.